

P-Hydrogen-Substituted 1,3,2-Diazaphosphenes: Molecular Hydrides

Sebastian Burck,[†] Dietrich Gudat,^{*†} Martin Nieger,[‡] and Wolf-Walther Du Mont[†]

Contribution from the Institut für Anorganische Chemie, Universität Stuttgart, Pfaffenwaldring 55, 70550 Stuttgart, Germany, Institut für Anorganische Chemie, Universität Bonn, Gerhard-Domagk-Strasse 1, 53121 Bonn, Germany, and Institut für Anorganische Chemie, Technische Universität Braunschweig, Hagenring 30, 38106 Braunschweig, Germany

Received November 30, 2005; E-mail: gudat@iac.uni-stuttgart.de

Abstract: *P*-Hydrogen-substituted 1,3,2-diazaphosphenes **1** were prepared by an improved procedure from diazadienes and were characterized by spectroscopy and in one case by X-ray diffraction. A unique hydride-type reactivity of the P–H bonds was documented by extensive reactivity studies. Aldehydes and ketones were readily reduced to diazaphospholene derivatives of the corresponding alcohols, with alkyl-substituted ketones being converted at much lower rates than aldehydes or diaryl ketones. Reactions with the tetrachlorides of group 14 elements proceeded via hydride/chloride metathesis to give either partially chlorinated derivatives $\text{EH}_n\text{Cl}_{4-n}$ ($n = 0-3$ for $\text{E} = \text{C}, \text{Si}$) or HCl and phosphonium salts **16c**[ECl_3] (for $\text{E} = \text{Ge}, \text{Sn}$) which were characterized by spectroscopic and X-ray diffraction studies. Tin dichloride was readily reduced to the element. Reactions of **1c** with the *P*-chloro-diazaphospholene **3c** and the salt **16c**[OTf] allowed the first experimental detection of intermolecular exchange of a hydride, rather than a proton, between phosphine derivatives. Computational studies indicated that the hydride transfer between **1c** and the cation **16c** involves a transient H-bridged species with bonding properties similar to those of B_2H_7^- . The preference for the formation of these bridged intermediates over P–P bonded phosphonium–phosphine adducts is attributed to the low electrophilicity of the diazaphospholenium cations and characterizes a novel reaction mode for phosphonium ions.

Introduction

Phosphine (PH_3), primary organophosphines (RPH_2), and secondary organophosphines (R_2PH) are distinguished by the presence of reactive phosphorus–hydrogen bonds whose capability to undergo chemical transformations makes these species widely used reagents and synthetic intermediates.¹ Many typical reactions involve formal conversion of the P–H into other P–E bonds (where E may be nearly any other metal or nonmetal) and occur via either metathetic replacement of a hydrogen or addition of a P–H bond to a carbon–carbon or carbon–heteroatom multiple bond (“hydrophosphination”). Several of these processes, e.g., the conversion into tertiary phosphines which are valuable ligands in many catalytic processes, are of considerable importance for both academic research and industrial chemistry.¹ From a mechanistic standpoint, substitution reactions are frequently carried out in the presence of strong bases,¹ whereas hydrophosphinations may proceed as radical processes under homolytic cleavage of the

P–H bond (Scheme 1a),^{1,2} as ionic reactions that are catalyzed by acids or bases,^{1,2} or under catalysis by transition metal complexes.³ Acid-catalyzed addition reactions of phosphines are presumed to proceed by nucleophilic attack of the phosphine on the substrate which was previously activated by the acid and subsequent deprotonation of the resulting phosphonium ion;^{2,4} in contrast, base-induced addition and substitution reactions are initiated by deprotonation of the phosphine by a catalytic or stoichiometric amount of base to give a phosphanide ($\text{R}_2\text{P}^-\text{M}^+$), which is then quenched by reaction with an electrophile or addition to a multiple bond.^{2,5} Both reaction mechanisms are in accord with the generally accepted concept of phosphines as weak acids (Scheme 1b).⁶

Since, as a consequence of the similar electronegativities of hydrogen ($\chi^{\text{AR}} 2.2$) and phosphorus ($\chi^{\text{AR}} 2.06$), the phosphorus–hydrogen bond lacks a pronounced polarity, it is conceivable that *P*-H-substituted phosphines can react not only as a source of radicals or as acids but also as hydride donors (Scheme 1c). An ambiguous behavior of this type is well established for

[†] Universität Stuttgart.

[‡] Universität Bonn.

^{*} Technische Universität Braunschweig.

(1) (a) Quin, L. D. *A Guide to Organophosphorus Chemistry*; Wiley-Interscience: New York, 2000. (b) Corbridge, D. E. C. *Phosphorus World 2005* (<http://www.phosphorusworld.com>). (c) *The Chemistry of Organophosphorus Compounds, Vol. 1*; Hartley F. R., Ed.; John Wiley & Sons: Chichester, 1990.

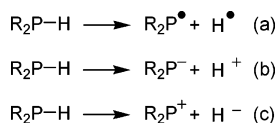
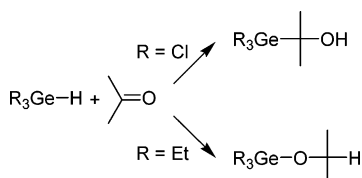
(2) Elsner, G. *Methoden der Organischen Chemie (Houben-Weyl)*, 1952–, 4th ed.; Georg Thieme Verlag: Stuttgart, 1980; Vol. 13/E1, p 122 ff.

(3) Baillie, C.; Xiao, J. *Curr. Org. Chem.* **2003**, *7*, 477.

(4) Rauhut, M. M.; Hechenbleikner, I.; Currier, H. A.; Schaefer, F. C.; Wystrach, V. P. *J. Am. Chem. Soc.* **1959**, *81*, 1103–1107.

(5) Hoff, M. C.; Hill, P. *J. Org. Chem.* **1959**, *24*, 356.

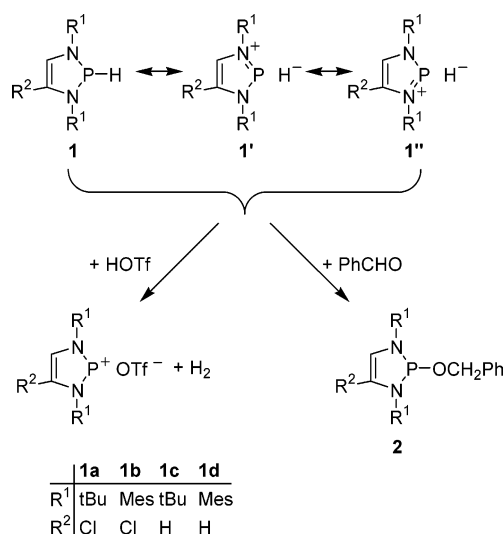
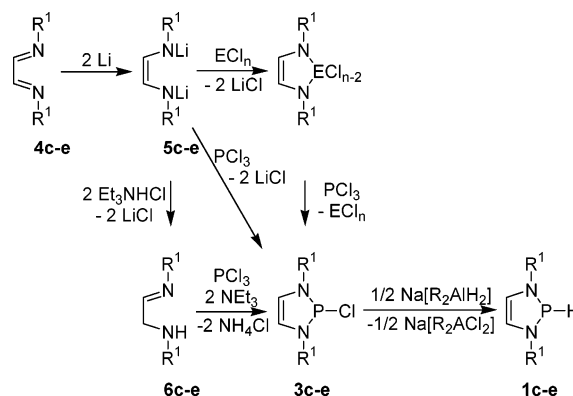
(6) Hudson, H. R. In ref 1c, p 473 ff.

Scheme 1. Possible Ways for Cleavage of P–H Bonds**Scheme 2**

hydrogermanes, where the electronegativity situation (χ^{AR} 2.02 for Ge) is similar;⁷ the polarity of the Ge–H bonds is generally low, and substituent influences or even special reaction conditions can have a determinative influence and may lead to a shift from radical to either “proton” or “hydride” reactivity. Such changes can have serious consequences on the outcome of reactions and may, e.g., result in an inverted regioselectivity (“Umpolung”), as exemplified in Scheme 2 for the addition of Et₃GeH and Cl₃GeH to carbonyl compounds, which can yield either a germylcarbinol (reflecting “proton” character of the Ge–H bond) or a germyl ether (reflecting “hydride” character of the Ge–H bond).⁷ A dualism between acidic and hydride character even in the presence of a somewhat larger electronegativity difference is likewise known for the reactions of Si–H bonds in silanes (χ^{AR} 1.74 for Si).⁸

That substituent-induced inversion of the E–H bond polarity is, in principle, also feasible in phosphorus compounds was first established by the observation of hydride-type reactivities for some hypervalent Lewis base adducts of phosphines.⁹ Some time ago, we described 2-H-diazaphospholenes **1** as the first three-coordinate phosphine derivatives showing “Umpolung” of the P–H bond polarity. This behavior is due to a hyperconjugative interaction between nonbonding π -electrons in the C₂N₂ unit and the $\sigma^*(\text{P}-\text{H})$ orbital (expressed by resonance between the canonical structures **1–1''**, Scheme 3), which induces a weakening of the P–H bond and an increase of negative charge density at the hydrogen atom.¹⁰ A preliminary survey of the chemical reactivity of **1** revealed that the hydride character became evident in the ability to react with acids under dehydrocoupling and to convert benzaldehyde into a benzyloxy-diazaphospholene **2** (Scheme 3), with concomitant reduction of the carbonyl to an alcohol function.¹⁰

Although the potential of phosphines as reducing agents has long been recognized,¹¹ the reaction of **1** is remarkable as it does not proceed—as usual—under deoxygenation of the substrate and conversion of the phosphine into a phosphine oxide, but rather via transfer of a hydride. Reactions involving reductive hydride transfer from phosphines to organic and main-group

Scheme 3**Scheme 4.** Synthesis of Diazaphospholenes^a

^a R = MeOCH₂CH₂; ECl_n = SiCl₄ or GeCl₂; R¹ = tBu (**1c–6c**), Mes (**1d–6d**), 2,6-*i*-Pr₂C₆H₃ (DIPP, **1e–6e**).

element compounds have as yet not been studied systematically. However, in consideration of the present knowledge on the reactivity of **1**, it is conceivable that further explorations in this field may lead to new applications for phosphines in organic and organometallic synthesis. This prospect stimulated us to evaluate the reactivity of the diazaphospholenes **1** toward various types of substrates in more detail. In this work, we will give a full account of the synthesis of 2-hydro-diazaphospholenes and a crystal structure study of one derivative, and we will report on a comprehensive investigation of the use of these species as hydride-transfer reagents toward organic carbonyl compounds, di- and tetrahalides of group 14 elements, and chlorophosphines.

Results and Discussion

Synthesis and Characterization of 2-Hydrido-1,3,2-diazaphospholenes. The P-hydrogen-substituted diazaphospholenes **1** are readily prepared via H/Cl exchange from the P-chloro-diazaphospholenes **3**.¹⁰ The latter are in turn accessible from readily available diazadienes **4** in a two- or three-step procedure (Scheme 4) involving (i) reduction of the starting material to a dilithium diazadienide salt **5** and (ii) either direct metathesis of this intermediate with PCl₃¹² or, alternatively,

- (7) Rivière, P.; Rivière-Baudet, M.; Satgé, J. In *Comprehensive Organometallic Chemistry*; Wilkinson, G., Stone, F. G. A., Abel, E. W., Eds.; Pergamon: Oxford, 1982; Vol. 2, p 399 ff.
 (8) Armitage, D. A. In ref 7, Vol. 2, p 1 ff.
 (9) (a) Carré, F.; Chuit, C.; Corriu, R. J. P.; Mehdi, A.; Reyé, C. *J. Organomet. Chem.* **1997**, 529, 59. (b) Bezombes, J.-P.; Carré, F.; Chuit, C.; Corriu, R. J. P.; Mehdi, A.; Reyé, C. *J. Organomet. Chem.* **1997**, 535, 81. (c) Alder, R. W.; Read, D. *Angew. Chem., Int. Ed.* **2000**, 39, 2879.
 (10) Gudat, D.; Haghverdi, A.; Nieger, M. *Angew. Chem., Int. Ed.* **2000**, 39, 3084.
 (11) (a) Buckler, S. A.; Doll, L.; Lind, F. K.; Epstein, M. *J. Org. Chem.* **1962**, 27, 794. (b) Studer, A.; Amrein, S. *Synthesis* **2002**, 835.

- (12) Carmalt, C. J.; Lomeli, V.; McBurnett, B. G.; Cowley, A. H. *Chem. Commun.* **1997**, 2095.

conversion of the diazadienide into a diazasilole¹³ or cyclic germylene¹² and subsequent ring metathesis with PCl_3 . The direct substitution pathway is clearly advantageous from a practical point of view, as it involves fewer and less time-consuming steps, but a drawback is that it provides only moderate yields of diazaphospholene (55% of **3c** by metathesis from **5c**¹²). In connection with our recent studies on the synthesis of *N*-heterocyclic arsenium and stibonium ions,¹⁴ we found now that the yields of chloro-diazaphospholenes **3** can be substantially improved when the dianions **5** are first quenched by protonation with Et_3NHCl and the resulting α -aminoaldimines **6** are then reacted with PCl_3 in the presence of NEt_3 as acid scavenger. Isolation of the intermediates **5**, **6** is not required so that the whole synthesis can be carried out in one pot. Using this protocol allows to prepare multigram quantities of the *N*-*tert*-butyl- and *N*-aryl-*P*-chloro-diazaphospholenes **3c–e** in one step from diazadienes with overall yields of 70–80%.

The completion of the synthesis of the target compounds **1c–e** from **3c–e** requires as the last step the replacement of the *P*-chloro-substituent by hydrogen. Although LiAlH_4 and LiBEt_3H have been initially employed for this purpose,¹⁰ their use suffers from the occurrence of side reactions (mainly cleavage of P–N bonds due to uncontrolled over-reduction) which reduce the yields and require extra efforts for the removal of the byproducts during workup. We have found that using a stoichiometric amount of sodium bis(methoxyethoxy)aluminum dihydride (“Red-Al”) for hydride transfer gives superior results by avoiding unspecific P–N bond cleavage and facilitating the separation of chloroaluminate salts by filtration. Following these protocols, pure *P*-hydrido-diazaphospholenes **1c–e** are easily isolated in yields of 50–70% after distillation (**1c**) or recrystallization (**1d,e**).

The pure diazaphospholenes **1c–e** are light yellow liquids (**1c**) or solids that are highly air and moisture sensitive. They are readily soluble in hydrocarbons, ethers, and acetonitrile but decompose when dissolved in protic solvents and in chlorinated hydrocarbons (see below). The composition and identity of all compounds were verified by analytical and spectroscopic data and in the case of **1e** by a single-crystal X-ray diffraction study. The spectroscopic data of **1c–e** display no peculiarities and are listed in detail in the Experimental Section. The structure of crystalline **1e** is composed of isolated molecules, without significant intermolecular interactions (Figure 1), whose individual features bear close similarity to those of the previously described 4-chloro-substituted diazaphospholene **1b**.¹⁰ As in that case, the five-membered ring exhibits a flat “envelope” conformation in which the phosphorus atom is out of the plane containing the other four ring atoms. The position of the hydrogen atom at phosphorus was located and refined freely using isotropic thermal displacement parameters, showing that the P–H bond takes on a flagpole position. The P–H distance of 1.48(1) Å is quite similar to that in **1b** (1.51(4) Å¹⁰) and likewise notably longer than known P–H bond lengths in phosphines (1.288 ± 0.09 Å¹⁵), and the endocyclic bond

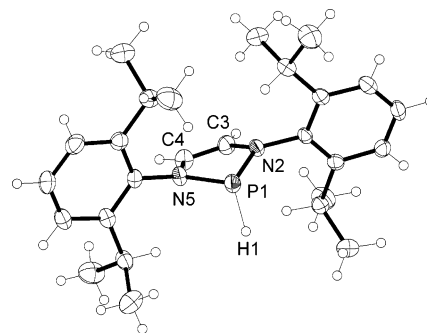


Figure 1. Molecular structure of **1e** in the crystal, ORTEP view. Thermal ellipsoids are at the 50% probability level. Selected bond lengths (in Å): P1–N5 1.691(1), P1–N2 1.712(1), P1–H1 1.48(1), N2–C3 1.408(2), N2–C6 1.437(2), C3–C4 1.317(2), C4–N5 1.416(2).

distances in **1e** (see caption to Figure 1) and **5** (P–N 1.709(3), 1.722(3); C–N 1.407(5), 1.410(5); C=C 1.327(5) Å¹⁰) are indistinguishable. The characteristic pattern of deviations from standard single- and double-bond distances has been interpreted as the result of hyperconjugation between the six π -electrons in the C_2N_2 unit and the $\sigma^*(\text{P–H})$ orbital and was stated as the dominant cause for the bond weakening and increased negative charge density at the hydrogen atom that account for the unique hydride nature of the P–H bonds in diazaphospholenes.¹⁰

Reactions with Carbonyl Compounds. Although the reductive dechlorination of phosgene is a well-established route for the preparation of phosphinous and phosphonous chlorides, R_2PCl and RPCl_2 , from primary and secondary phosphines,² the latter react with aldehydes and ketones not by reduction of the carbonyl group but via P–C bond formation to give α -phosphino-carbinols. Having discovered¹⁰ the reduction of benzaldehyde by **1b** (Scheme 3) as a remarkable exception to this behavior, we wanted to evaluate the scope and limitation of this reaction as a new approach to the reduction of organic carbonyls. For this purpose we set out to study the behavior of the diazaphospholene **1c**, which was chosen as the synthetically most easily accessible derivative, toward a larger range of substrates. Additional sampling experiments revealed that **1d,e** behave very much the same way as **1c**, whereas the reactions of **1a,b** were in some cases complicated by side reactions involving the 4-chloro substituents (see below).

The reactions of **1c** with aldehydes (2-methoxybenzaldehyde, butyraldehyde) and benzophenone were completed within a couple of minutes at ambient temperature (as judged by the fading of the orange color of the starting material) and proceeded, like the reaction of **1b** with benzaldehyde, with reduction of the carbonyl function to yield the diamidophosphinites **8–10** (Scheme 5) along with varying amounts (<5–25%) of the phosphorous acid diamide **7**; the formation of the latter is explained by reaction of **1c** with traces of water present in the reaction.¹⁶ Reaction of **1c** with cinnamaldehyde afforded the 1,4-addition products **11a,b** as a 3:1 mixture of *E/Z* stereoisomers, together with a small amount of **7**; the allylic alcohol derivative **12**, resulting from formal 1,2-addition of the phosphine to the carbonyl moiety, was not detectable. The benzylic derivatives **8** and **10** were isolated as colorless, crystalline solids after workup of the reaction mixtures and were characterized by analytical and spectroscopic data, whereas **9**

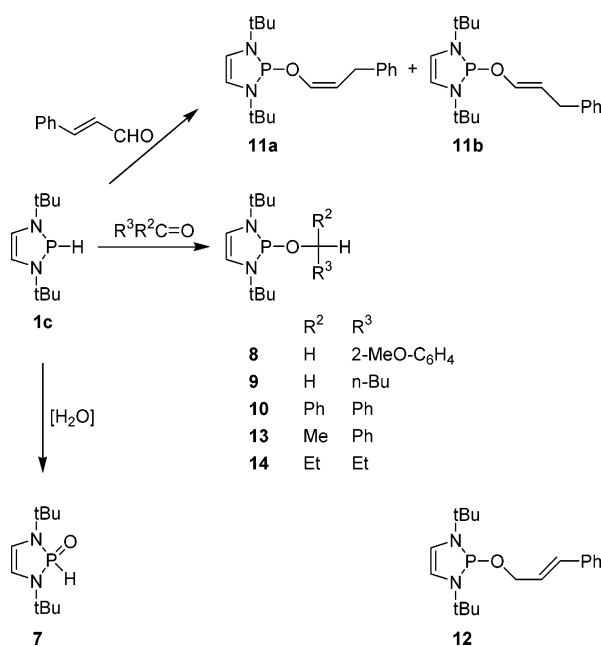
(13) Denk, M. K.; Gupta, S.; Ramachandran, R. *Tetrahedron Lett.* **1996**, 37, 9025.

(14) (a) Gudat, D.; Gans-Eichler, T.; Nieger, M. *Chem. Commun.* **2004**, 2434. (b) Gudat, D.; Gans-Eichler, T.; Nieger, M. *Heteroat. Chem.* **2005**, 16, 327.

(15) Average and standard deviation as the result of a query in the CSD database for P–H distances in three-coordinate phosphorus compounds $\text{H}_n\text{Y}_{3-n}\text{P}$ (Y = substituent bound via a p-block element).

(16) Burck, S.; Gudat, D.; Nieger, M. *Angew. Chem., Int. Ed.* **2004**, 43, 4801.

Scheme 5

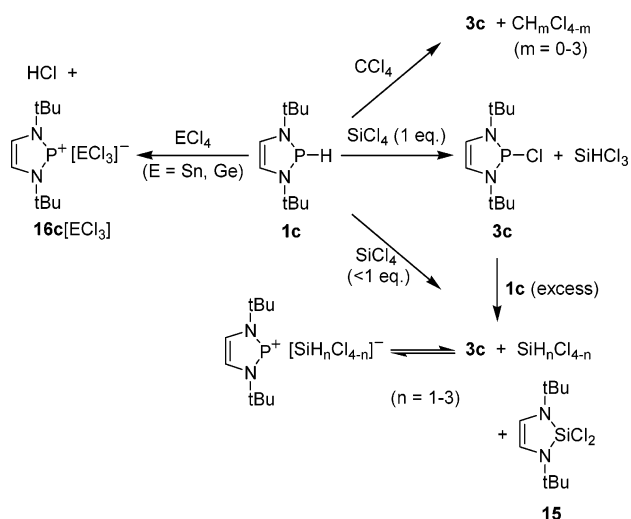


and **11a,b** were unambiguously identified from the analysis of multinuclear and multidimensional NMR spectra of the reaction mixture (in these cases, reactions were performed in NMR tubes using C_6D_6 as solvent), but no attempts were made to isolate them. Assignment of the position and configuration of the double bond in **11a,b** is based on the values of $^nJ_{HH}$ and $^nJ_{PH}$ coupling constants involving the hydrogen atoms in the double bond and the adjacent CH_2 moiety; not surprisingly, the values obtained match closely the analogous couplings in the corresponding free enols.¹⁷

The analogous reactions of **1c** with acetophenone (45% conversion after 12 h at ambient temperature) and diethyl ketone (approximately 8% conversion after 12 h at ambient temperature) proceeded at much lower rates, and NMR signals of unreacted starting materials remained visible over a period of several days at ambient temperature. Although no attempts to isolate individual products were made, NMR studies on the reaction mixtures allowed us to establish unambiguously the formation of the expected diamidophosphinites **13**, **14** and the hydrolysis product **7**, and to disprove the presence of further spectroscopically detectable side products or intermediates. Monitoring the time-dependent changes of signal intensities revealed that the fraction of **7** increased substantially during later stages of the reaction, suggesting that its formation arises most likely from slow diffusion of traces of water into the NMR tubes. In contrast to the reactions with aldehydes and ketones, **1c** was found to be unreactive toward esters such as ethyl acetate and methyl benzoate.

Reactions with Chlorides of Group 14 Elements. The ability of the diazaphospholenes **1** to effect reductive dechlorination of organic halides was discovered serendipitously when it was noted that attempts to dissolve **1b** in CH_2Cl_2 resulted in formation of the 2-chloro-diazaphospholene **3d**¹⁰ and that reactions of **1b** with olefins or carbonyls were often accompanied by the formation of **3d** as a side product. While the fate of the hydrogen atom in the first reaction remained

Scheme 6



unknown, the conversion of **1b** into **1d** can be rationalized as P–H/C–Cl bond metathesis involving the transfer of a hydride from a phosphorus to a carbon atom. To elucidate the suitability of diazaphospholenes **1** as hydride-transfer reagents on a broader scale, we initiated a detailed study of the reactions of **1c** with ECl_4 ($E = C, Si, Ge, Sn$) and ECl_2 ($E = Ge, Sn$), respectively.

The reaction of CCl_4 with 1 equiv of **1c** at room temperature was instantaneous and afforded the *P*-chloro-diazaphospholene **3c** and a mixture of chloromethanes CH_mCl_{4-m} ($m = 0-3$), which were identified in situ by 1D and 2D NMR spectroscopy (Scheme 6). Addition of **1c** in excess resulted in eventual consumption of CCl_4 and formation of CH_2Cl_2 and CH_3Cl as main products. In contrast to the unselective reaction with CCl_4 , reduction of $SiCl_4$ with 1 equiv of **1c** gave **3c** and $SiHCl_3$ as the only products identifiable by NMR spectroscopy; both species were not isolated. Further reaction with an excess of **1c** (1–2 molar equiv) was unselective, and NMR studies of the reaction mixture disclosed the presence of unreacted $SiHCl_3$ in addition to three new silicon-containing products. The two major components showed characteristic 1H and ^{29}Si signals which led to their assignment as the anticipated reaction products, SiH_2Cl_2 and SiH_3Cl , even though the observed chemical shifts and couplings differ markedly from the reported data for these compounds.¹⁹ The origin of this divergence is attributable to the presence of rapid (on the NMR time scale) dynamic chloride exchange between the halosilanes and **3c** (see Scheme 6); the observed chemical shifts and couplings under these conditions represent a population-weighted average of the data of SiH_nCl_{4-n} and the silicates $[SiH_nCl_{5-n}]^-$, and it was feasible to demonstrate that changing the composition of the solution by adding either **3c** or a mixture of silanes SiH_nCl_{4-n} (prepared by partial reduction of $SiCl_4$ with $LiAlH_4$) shifted the positions of all 1H , ^{31}P , and ^{29}Si NMR signals and the magnitude of $^1J_{SiH}$ couplings. From the size of these shifts it can be concluded that the chloride affinity increases in the order $SiHCl_3 < SiH_2Cl_2 < SiH_3Cl$. Chloride abstraction from **3c** by $GeCl_4$ had previously been demonstrated.¹²

The third product of the reaction of $SiCl_4$ with **1c** (formed in yields <5%) was distinguished by the absence of Si–H bonds

(17) Bergens, S. H.; Bosnich, B. *J. Am. Chem. Soc.* **1991**, *113*, 958.

(18) tom Dieck, H.; Zettlitzer, M. *Chem. Ber.* **1987**, *120*, 795.

(19) Löwer, R.; Vongehr, H.; Marsmann, H. C. *Chem. Z.* **1975**, *99*, 33.

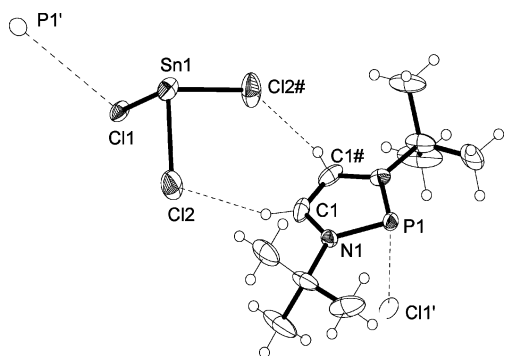


Figure 2. Molecular structure of **16c**[SnCl₃] in the crystal, ORTEP view. Thermal ellipsoids are at the 50% probability level. Atoms P1' and Cl1' of neighboring ions and intermolecular contacts are depicted as dashed lines. Selected bond lengths (in Å) and angles (in deg; values for **16c**[GeCl₃] in brackets): P1–N1 1.660(2) [1.664(1)], N1–C1 1.363(3) [1.367(2)], C1–C1# 1.336(5) [1.339(4)], Sn1–Cl1 2.453(1) [Ge1–Cl1 2.282(1)], Sn1–Cl2 2.470(1) [Ge1–Cl2 2.308(1)], Cl1–Sn1–Cl2 93.60(2) [Cl1–Ge1–Cl2 95.91(2)], Cl2#–Sn1–Cl2 95.56(3) [Cl2#–Ge1–Cl2 97.32(3)].

and was identified as the known diazasilole **15**¹⁸ by comparison of its spectral data with those of an authentic sample. The formation of **15** is explained by ring metathesis between **3c** and SiCl₄ (or the reduction products SiH_nCl_{3–n}) under formal exchange of the PCl for an SiCl₂ moiety; this reaction is the reversal of the previously reported metathesis between **15** and SiCl₄ which had been utilized in the first synthesis of **3c**.¹³

The reactions of GeCl₄ and SnCl₄ with equimolar amounts of **1c** afforded quantitative yields of the appropriate phosphonium trichlorogermanate or trichlorostannate, **16c**[ECl₃] (E = Ge, Sn). The formation of HCl as byproduct was proven by its trapping as hydrochloride after addition of diazabicyclo[2.2.2]-octane (DABCO). The salts **16c**[ECl₃] were isolated as light yellow crystalline solids and were characterized by analytical and spectroscopic data and single-crystal X-ray diffraction studies. The crystals of both compounds are isomorphous (space group *Pnma*) and consist of pairs of anions and cations (see Figure 2) that lie on a crystallographic mirror plane. The ions in each pair are connected by weak hydrogen bonds between two chlorine atoms and the hydrogen atoms on the double bond (Cl2–H1 2.63 Å). The third chlorine atom displays an additional contact to the phosphorus atom of an adjacent ion pair (P···Cl 3.45 (**16c**[SnCl₃]), 3.39 (**16c**[GeCl₃]) Å) which is slightly shorter than the sum of van der Waals radii (3.55–3.75 Å) and may be interpreted in favor of a weak intermolecular Lewis acid–base interaction. If one considers both types of intermolecular interactions, the crystal packing can be described in terms of one-dimensionally infinite zigzag chains of alternating and weakly interacting anions and cations. The molecular structure of individual cations **16c** is characterized by planar five-membered rings whose endocyclic bond distances (cf. Figure 2) and angles are, within experimental error, indistinguishable from each other and from those in other known diazaphospholenium salts.^{12,20,21} The anions show slightly distorted (with respect to local C_{3v} symmetry) trigonal pyramidal structures whose bond lengths and angles (Figure 2) match the data of other salts with the same anions.²²

Treatment of the phosphonium salts **16c**[ECl₃] with an excess of **1c** resulted in exothermic reactions which proceeded under gas evolution and immediate formation of orange (E = Ge) or black (E = Sn) insoluble precipitates. The supernatant solutions contained the *P*-chloro-diazaphospholene **3c** as the only spectroscopically detectable phosphorus-containing species. Identical products were obtained when **16c**[ECl₃] were replaced by GeCl₂ × dioxane, or SnCl₂, respectively. More detailed studies of the reactions involving **16c**[SnCl₃] and SnCl₂ disclosed that complete conversion of the starting materials required 1 molar equiv of **1c** and that the black precipitate consisted of elemental tin and led thus to the formulation of the overall reaction as **1c** + SnCl₂ → **3c** + Sn + HCl.

In light of the previous findings and the results of Schlecht,²³ who obtained elemental germanium as an orange solid by reduction of GeCl₂ × dioxane with Li[BET₃H], it was expected that the same product might be formed by reduction of GeCl₂ or **16c**[GeCl₃] with **1c**. Even though a powder diffraction study confirmed that the insoluble orange material obtained indeed contains germanium, the diffraction pattern showed additional peaks, and elemental analysis revealed the presence of substantial amounts (>30%) of organic material. Furthermore, samples from different batches deviated perceptibly in their composition. As solid-state NMR studies allowed us to identify the cation **16c** as a constituent of the solid, we conclude that the orange material is a mixture of germanium with an ionic phase which is composed of the cation **16c** and a subvalent, presumably oligomeric or polymeric, germanate anion of yet unknown structure. Attempts to characterize the material obtained in more detail are still in progress.

In comparing the reactivity of **1c** toward different tetrahalides, it appears at first glance that the reactions with CCl₄ and SiCl₄ (which proceed via *substitution* at the group 14 element) take a different course than those with GeCl₄ and SnCl₄ (which proceed via *reduction* of the group 14 element). Nonetheless, all processes can be rationalized by a common mechanism if one considers that **1c** behaves as a hydride donor and reacts with all starting materials via E–Cl/P–H bond metathesis to give **3c** and EHCl₃ as initial products. The latter may then decay via two competing reaction channels, undergoing either reductive elimination of hydrogen chloride to yield the dichlorides ECl₂ or subsequent metathesis of further E–Cl bonds under consumption of more equivalents of **1c**. The second alternative is obviously preferred for the carbon and silicon halides, which undergo reductive elimination to transient dichlorocarbenes or -silylenes only in the presence of strong bases²⁴ and were found to react with excess **1c** under successive metathesis of up to three of four E–Cl bonds. It remains presently undecided if the last chlorine atom is not replaced at all, or if the tetrahydrides EH₄ (E = C, Si) evade spectroscopic detection because of their high volatility. In contrast to their lighter homologues, GeHCl₃ and SnHCl₃ are known to coexist in donating solvents in equilibrium with ECl₂ and HCl.²⁵ The dihalides formed in this reductive elimination are Lewis acids that may react with **3c** under chloride abstraction, as was autonomously verified by the independent synthesis of **16c**[ECl₃] from **3c** and ECl₂, and

(20) Gudat, D.; Haghverdi, A.; Hupfer, H.; Nieger, M. *J. Eur. Chem.* **2000**, *6*, 3414.

(21) Denk, M. K.; Gupta, S.; Lough, A. J. *Eur. J. Inorg. Chem.* **1999**, 41.

(22) Average and standard deviation as the result of a query in the CSD database for trichlorostannates and trichlorogermanates: Sn–Cl, 2.51 ± 6 Å; Cl–Sn–Cl, 92 ± 3°; Ge–Cl, 2.30 ± 3 Å; Cl–Ge–Cl, 95.6 ± 1.5°.

(23) Schlecht, S. *Angew. Chem., Int. Ed.* **2002**, *41*, 1178.

(24) Karsch, H. H.; Schlüter, P. A.; Bienlein, F.; Herker, M.; Witt, E.; Sladek, A.; Heckel, M. *Z. Anorg. Allg. Chem.* **1998**, *624*, 295.

(25) *Inorganic Reactions & Methods*; Zuckerman, J. J., Ed.; VCH Publishers: New York, 1989; Vol. 3, p 399 ff and references cited therein.

the coupling of both equilibria can explain the quantitative formation of these salts in the reaction of **1c** with ECl_4 . Reaction of excess of **1c** under these circumstances must occur with the divalent chlorides rather than with EHCl_3 , and it can be envisaged that, for $\text{E} = \text{Sn}$, the reaction is completed by another sequence of hydride-transfer and reductive elimination steps to yield Sn , HCl , and a second equivalent of **3c**.

Reactions with Chlorophosphines. Whereas **1c** did not react with phosphorus trichloride in a controlled way, the reaction with diphenylchlorophosphine afforded diphenylphosphine and **3c** as the only NMR spectroscopically detectable products. This process boils down to the interconversion between two phosphine derivatives via exchange of chloride and hydride substituents and is practically irreversible, as the products must be considered thermodynamically more stable than the starting materials.²⁶ We wondered if similar reactions might likewise be feasible under reversible hydride transfer. As it was anticipated that a reversible process is most easily observable in a degenerate reaction where the thermodynamic driving force is zero and mechanistic information is often conveniently available from dynamic NMR, we decided to investigate first the reaction of **1c** with **3c**. ^1H and ^{31}P NMR spectra of mixtures of both species in CD_3CN at ambient temperature displayed a distinct broadening of all signals as compared to the spectra of solutions of the pure compounds. The interpretation of this effect as dynamic line broadening arising from slow (on the NMR time scale) chemical exchange was confirmed by a 2D ^1H EXSY experiment (Figure 3a). The presence of intermolecular correlations connecting the signals of olefinic and aliphatic hydrogen atoms of both reactants proved unambiguously that the two species are in dynamic equilibrium and undergo reversible H/Cl exchange on a second time scale.

Evidence for reversible hydride transfer was observed as well when **3c** was replaced by an ionic diazaphospholenium triflate. Samples prepared by dissolution of equimolar amounts of **1c** and **16c**[OTf] in CD_3CN at ambient temperature showed a single broad ^{31}P NMR signal (Figure 3c) which sharpened somewhat when the spectrum was recorded at higher temperatures. The ^1H NMR spectrum at ambient temperature displayed a single set of sharp resonances for the olefinic and aliphatic hydrogen atoms of both components and an additional singlet for the *P*-bound hydrogen atom (Figure 3b). The spectral features are consistently interpreted by assuming that intermolecular scrambling of a hydride between the two reactants occurs at a rate at (or close to) the fast exchange limit; this leads to coalescence of the separate signals of the phosphorus and the aliphatic and olefinic hydrogen atoms of both components and a collapse of the doublet splitting of the signal of the *P*-bound hydrogen atom in **1c** due to the scalar coupling via $^1J_{\text{PH}}$. Cooling to approximately $-30\text{ }^\circ\text{C}$ led to broadening of all lines, in accord with the expectation of the exchange slowing down with decreasing temperature. At still lower temperatures, the salt **16c**[OTf] precipitated and the signals of **1c** reappeared in the spectrum of the supernatant solution, confirming that the original components were still present and had not reacted to a new product. All changes were completely reversible upon warming the sample again to ambient temperature. The chemical shifts in the NMR spectra of mixtures of **1c**/**16c**[OTf] always comply with the value of the population-weighted average of the shifts

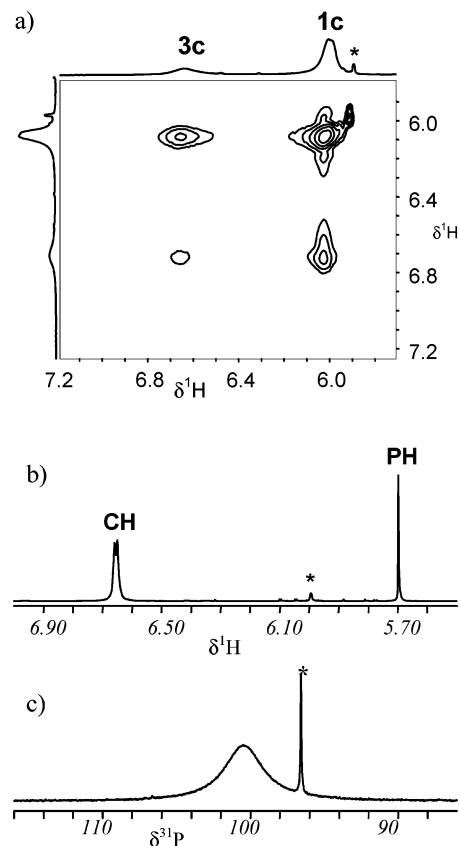
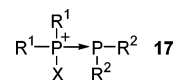


Figure 3. (a) Expansion of the olefinic region of a 2D ^1H EXSY spectrum of a mixture of **3c** and **1c** in CD_3CN . The traces on top and left of the 2D spectrum depict the ^1H NMR spectrum of the same solution. The off-diagonal correlations connecting the peaks of both reactants in the 2D map prove clearly the presence of dynamic exchange during the mixing time ($\tau = 500\text{ ms}$). (b,c) Expansion of the ^1H (b) and ^{31}P (c) NMR spectra of an equimolar mixture of **1c** and **16c**[OTf] in CD_3CN . The signals of the olefinic and the PH protons are denoted with CH and PH, respectively. The signals marked with asterisks are attributable to an impurity arising from hydrolytic decomposition of the reactants.

Chart 1



of the pure compounds, which suggests that noticeable amounts of transient intermediates are not involved. Even though no precise rate constants could be extracted, the NMR spectra indicate that interconversion between **1c** and the chlorophosphine **3c** is slower than that between **1c** and the cation **16c**.²⁷

The reversible intermolecular transfer of a hydride from a phosphine to a phosphonium ion, although conceptually straightforward, must still be regarded as a remarkable process, as it is in sharp contrast to the established reaction pattern, viz. the formation of P–P bonded adducts of the type **17** (Chart 1) via dative interaction of the lone-pair of the phosphine (a Lewis base) with the vacant orbital of the phosphonium cation (a Lewis acid).^{28,29} Even though the P–P bond formation is reversible and labile phosphonium–phosphine adducts may easily dis-

- (27) A dynamic exchange similar to that for **1c**/**16c**[OTf] was also observed between the *P*-chloro-diazaphospholenes **3c–e** and **16c–e**[OTf], suggesting that these species equilibrate in a similar way via intermolecular chloride scrambling. A detailed discussion of this reaction will be given elsewhere.
 (28) (a) Schultz, C. W.; Parry, R. W. *Inorg. Chem.* **1976**, *15*, 3046. (b) Cowley, A. H.; Lattman, M.; Wilburn, J. C. *Inorg. Chem.* **1981**, *20*, 2916. (c) Abrams, M. B.; Scott, B. L.; Baker, R. T. *Organometallics* **2000**, *19*, 4944.

(26) Gudat, D. *Eur. J. Inorg. Chem.* **1998**, 1087.

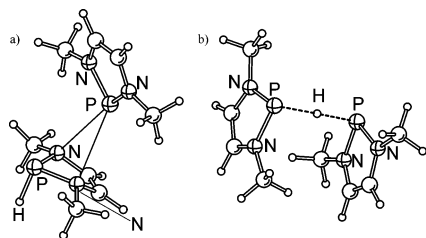


Figure 4. Representation of the computed molecular structures of **18** (a), **19-C₂** (b). Intermolecular contacts in **18** are drawn as thin lines. Relevant distances are listed in Table 1.

sociate into the free fragments²⁸ or partake in exchange reactions with other phosphines,²⁹ they tend to retain unsymmetric molecular structures and refrain from undergoing 1,2-shifts of substituents at the phosphorus atoms.^{28,29} In view of these considerations and the incompatibility of the NMR data of known phosphonium–phosphine adducts with the spectral data of the exchanging solutions of **1c/16c**[OTf], it appears highly likely that the hydride-transfer reactions involve adducts of the type **17** neither as stable products nor as transient intermediates.

To obtain mechanistic insight into the hydride exchange and possibly to understand why this reaction is preferred over the formation of P–P bonded adducts, we performed computational studies of the reactions of diazaphospholenium ions with diazaphospholenes. As **16**[OTf] exists in solution as a solvent-separated ion pair,²⁰ we focused on modeling the interaction of the *P*-H-diazaphospholene **1g** with the isolated cation **16g**. In both species, the bulky *N*-*tert*-butyl or *N*-aryl groups were downsized to methyl substituents in order to reduce the cost of the calculations. All computations, including the calculations of harmonic vibrational frequencies and zero-point energies (ZPE), were performed at the B3LYP/6-31+g** level; single-point energy calculations were further carried out at the given geometries using more extended 6-311+g(2d,p) basis sets. The assignment of a structure as a local minimum or transition state on the potential energy hypersurface was established by analysis of the second derivatives (minima have no and transition states have one negative eigenvalue of the Hessian matrix).

Attempts to determine an energy-optimized geometry for a P–P bonded adduct between **16g** and **1g** did not lead to the localization of a stable bonded structure but ended inevitably in fragmentation, giving rise to a supramolecular complex **18** (Figure 4a). The bond distances and angles in each fragment and the charge distributions obtained from NBO analyses³⁰ are closely similar to those computed for free **1g** and **16g** at the same level of theory (Table 1). The shortest intermolecular contacts of 3.17 and 3.22 Å are found not between the two phosphorus atoms, as would be expected for a phosphonium–phosphine adduct, but between the phosphorus atom of the cationic fragment and the nitrogen atoms of the neutral fragment. As according to the NBO results these atoms carry the largest positive and negative atomic charges, it appears that the assembly of the supermolecule **18** is charge controlled, and the sizable gain in energy of $\Delta E_{\text{ZPE}} = -10.0 \text{ kcal mol}^{-1}$ ($\Delta E_{\text{ZPE}} = E_{\text{ZPE}}(\mathbf{18}) - E_{\text{ZPE}}(\mathbf{1g}) - E_{\text{ZPE}}(\mathbf{16g})$) at the B3LYP/6-31+g** level

Table 1. Computed Relative Energies (in kcal mol⁻¹ at the B3LYP/6-31+g(d,p) Level of Theory) and Important Bond Lengths of **1g**, **16g**, and the Molecular Adducts **18** and **19**

	1g	16g	18	19-C₂	19-C₁
symmetry	<i>C_s</i>	<i>C_{2v}</i>	<i>C₁</i>	<i>C₂</i>	<i>C₁</i>
ΔE^a			-10.7 (-10.3)	-11.9 (-11.2)	-11.9 (-11.2)
ΔE_{ZPE}			-10.0	-13.5	-13.3
ΔG^{298}			-1.0	-2.1	-3.1
P–N	1.747	1.695	1.760 ^b 1.763 ^b 1.703 ^c 1.702 ^c	1.709, 1.711	1.711 ^b 1.713 ^b 1.707 ^c 1.709 ^c
N–C	1.413	1.367	1.412 ^b 1.414 ^b 1.373 ^c 1.373 ^c	1.389, 1.391	1.391 ^b 1.393 ^b 1.388 ^c 1.389 ^c
C=C	1.348	1.373	1.349 ^b 1.367 ^c	1.358	1.358 ^b 1.359 ^c
P–X	1.480		1.462	1.771	1.716 ^b 1.834 ^c

^a Values in parentheses denote energies calculated with 6-311+g(2d,p) basis sets at the energy-optimized molecular geometry obtained at the B3LYP/6-31+g(d,p) level. ^b Diazaphospholene unit. ^c Diazaphospholenium cation unit.

with inclusion of zero-point energy but uncorrected for basis set superposition error³¹) upon association presumably reflects the electrostatic (ion–dipole) interaction between the two molecular fragments.

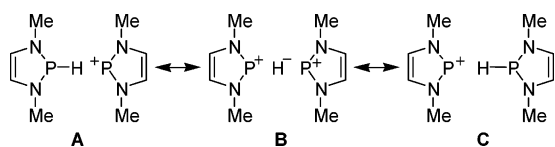
As the orientation of the fragments in the dimer **18** is unsuitable for intermolecular hydride transfer, we looked for a conformation with a closer contact of the P–H bond to the phosphonium center. This search resulted in the identification of a structure **19-C₂** (Figure 4b), which can be described as a *C₂*-symmetric assembly of two diazaphospholenium moieties that are connected by a symmetric P–H–P bridge. The endocyclic bond lengths range between those reported for cationic **16g** and neutral **1g** (Table 1). The phosphorus and the bridging hydrogen atom form a quasilinear assembly (P–H–P 179.1°). The P–H distances (1.771 Å) are clearly longer than in **1g** (1.480 Å) and indicate significant bonding interaction between all three atoms. Although **19-C₂** is even lower in energy than **18** ($\Delta E_{\text{ZPE}} = -13.5 \text{ kcal mol}^{-1}$ vs **1g/16g**³¹), the analysis of the second derivatives disclosed a negative eigenvalue of the Hessian matrix that is associated with a motion of the bridging hydride along the P–P vector, suggesting that **19-C₂** is a possible transition state of a hydride-transfer reaction. Further energy optimization without symmetry constraints allowed us finally to identify a molecular structure **19-C₁** with an unsymmetrical P–H–P bridge as a local minimum on the energy hypersurface. The dislocation of the bridging hydrogen atom lengthens one P–H bond to 1.834 Å; the second bond shortens to 1.716 Å but stays clearly longer than the P–H distance in **1g** computed at the same level of theory (1.480 Å). The bond lengths and angles in the diazaphospholene moieties (Table 1) and the P⋯P distance (3.542 Å in **19-C₂** vs 3.550 Å in **19-C₁**) remain essentially unaffected. Quite interestingly, the energies of **19-C₂** and **19-C₁** are virtually identical (see Table 1) and differ still by less than 0.2 kcal mol⁻¹ when zero-point energies are included. NBO population analyses reveal a marked increase of negative atomic charge on the P-bound hydrogen

(29) (a) Burford, N.; Cameron, T. S.; Ragogna, P. J. *J. Am. Chem. Soc.* **2001**, *123*, 7947. (b) Burford, N.; Ragogna, P. J.; McDonald, R.; Ferguson, M. J. *J. Am. Chem. Soc.* **2003**, *125*, 14404.

(30) Glendening, E. D.; Badenhoop, J. K.; Reed, A. E.; Carpenter, J. E.; Bohmann, J. A.; Morales, C. M.; Weinhold, F. *NBO 5.0*; Theoretical Chemistry Institute: University of Wisconsin, Madison, 2001 (<http://www.chem.wisc.edu/~nbo5>).

(31) Attempts to estimate the basis set superposition error by using a counterpoise correction led to corrected energies of $\Delta E_{\text{ZPE,corr}} = -9.0 \text{ kcal mol}^{-1}$ for **18** and $-12.3 \text{ kcal mol}^{-1}$ for **19-C₂**.

Chart 2



atom in both species ($q(\text{H}) = -0.21$) and a decrease of the Wiberg bond index (WBI) for the P–H bonds (WBI = 0.48/0.37 in **19-C**₁ and 0.43 in **19-C**₂) as compared to the values for **1g** ($q(\text{H}) = -0.13$; WBI = 0.88). Inspection of the natural bond orbitals and a second-order perturbation theory analysis of the Fock matrix in the NBO basis suggest a description of the P...H...P bonding as a three-center, two-electron bond that is formed by interaction of the electron pair of the P–H bond with the empty p-orbital of the phosphonium center and may be represented as shown in Chart 2 by resonance between canonical structures **A**–**C**. Although such electron-deficient single-hydride bridges are not common, they have precedence in the chemistry of main-group hydrides,³² and **19** may be regarded as isolobal to species like $[\text{B}_2\text{H}_7]^-$ ³³ and $[\text{Me}_3\text{AlHAL-Me}_3]^-$.³⁴ It should be noted that asymmetric hydride bridges had been encountered in an earlier computational study on $[\text{B}_2\text{H}_7]^-$,³⁵ although it was later shown that this effect depended highly on the quality of the basis set and the presumption that the potential hypersurface was very flat.³⁶ Considering these results, it remains unclear whether the unsymmetrical hydride bridge in **19-C**₁ is real or merely an artifact of the theoretical model employed.

In assessing the significance of the computational results, it must be conceded that a comprehensive account of the molecular dynamics is unfeasible as long as the influences of counterions and solvation are excluded. Questions as to precise activation energies or the symmetrical or unsymmetrical nature of a hydride-bridged intermediate must thus remain open. However, in the light of the present results and the known capability of diazaphospholenes to form stable transition metal complexes³⁷ and borane adducts,¹⁰ we conclude that the preference for substituent exchange over the formation of phosphine–phosphonium is attributable to the outstandingly low Lewis acidity of the diazaphospholenium ions^{10,26} rather than to insufficient nucleophilicity of the diazaphospholene component.

Conclusions

An efficient protocol for the synthesis of *P*-hydrido-1,3,2-diazaphospholenes **1** from diazadienes via the *P*-chloro derivatives **3** has been developed. Extensive studies of the reaction behavior confirmed that the compounds **1** behave as molecular hydrides that reduce organic carbonyl compounds and undergo halide/hydride metathesis with halides of various main-group elements. These reactions resemble those of complex hydrides such as NaBH_4 or LiAlH_4 but are set apart by the good solubility of the molecular hydrides, which permits reductions in nonpolar hydrocarbon solvents, and a retarded reactivity, which causes,

e.g., alkyl ketones to be reduced at significantly lower rates than diaryl ketones or aldehydes and permits the selective partial reduction of SiCl_4 to SiHCl_3 or of germanium and tin tetrachloride to the dichlorides. In this, the compounds **1** show a remarkable substrate selectivity which makes them potentially useful reagents in organic or organometallic synthesis for controlled reduction of multifunctional molecules. Possible applications in the deposition of metal films from hydrocarbon solutions, as well as the selective synthesis of new Ge(II) species are currently under study.

Apart from synthetic applications, the observed reversible hydride exchange between **1** and neutral chloro-diazaphospholenes or diazaphospholenium cations is of particular interest from a mechanistic point of view. Although computed energies of isodesmic hydride exchange reactions with phosphines have been previously considered as a means to assess relative stabilities of phosphonium cations,³⁸ these reactions are now, for the first time, established by experiment. Computational studies suggest that the transfer involves a transient hydride-bridged intermediate whose bonding is closely related to that of species such as $[\text{B}_2\text{H}_7]^-$. The preference for the formation of H-bridged dimers over the formation of P–P bonded Lewis acid–base adducts is further unprecedented for phosphonium ions. A reasonable explanation for this behavior can be given by considering the extraordinarily low electrophilicity of the cations, which disfavors an orbital-controlled reaction (formation of a dative P–P bond) over a charge-controlled reaction (formation of X-bridged adducts with a high degree of ionic bonding).

Experimental Section

General Remarks. All manipulations were carried out under dry argon. Solvents were dried by standard procedures. NMR spectra were obtained on a Bruker Avance 400 instrument (^1H , 400.1 MHz; ^{13}C , 100.5 MHz; ^{31}P , 161.9 MHz) at 303 K. Chemical shifts are referenced to external TMS (^1H , ^{13}C), 85% H_3PO_4 ($\Xi = 40.480747$ MHz, ^{31}P), Me_4Si ($\Xi = 19.867187$ MHz, ^{29}Si), or Me_4Sn ($\Xi = 37.290632$ MHz, ^{119}Sn). Coupling constants are given as absolute values. The prefixes i, o, m, and p denote atoms of *N*-aryl substituents. Mass spectrometric data were collected on a Varian MAT 711 instrument in EI mode at 70 eV. Elemental analyses were conducted with a Perkin-Elmer 2400CHSN/O analyzer. Melting points were determined in sealed capillaries.

Computational Studies. DFT calculations were carried out with the Gaussian 03 program suite³⁹ using Becke's three-parameter exchange functional with a Lee–Yang–Parr correlation energy functional (B3LYP) and split-valence basis sets of double- ξ quality augmented by one set of polarization functions on all atoms and diffuse functions on all heavy atoms (6-31+g(d,p)). Harmonic vibrational frequencies and zero-point energies were calculated at the same level. All structures reported are minima (only positive eigenvalues of the Hessian matrix) or transition states (one negative eigenvalue) on the potential energy surface. Single-point energy calculations were also carried out with 6-311+g(2d,p) basis sets at the given geometries. Analyses of electron populations were carried out with the NBO 5.0 module.³⁰ Listings of atomic coordinates and absolute energies are given as Supporting Information.

General Procedures for the Preparation of the 2-Chloro-1,3,2-diazaphospholenes 3. (a) From α -Aldimino-aldimines. The appropri-

(32) Treboux, C.; Trinquier, G. *Inorg. Chem.* **1992**, *31*, 4201.

(33) Watkins, M. I.; Bau, R. *J. Am. Chem. Soc.* **1982**, *104*, 7670.

(34) Atwood, J. L.; Hrnčir, D. C.; Rogers, R. D.; Howard, J. A. K. *J. Am. Chem. Soc.* **1981**, *103*, 6787.

(35) Sapse, A.-M.; Osorio, L. *Inorg. Chem.* **1984**, *23*, 627.

(36) Raghavachari, K.; Schleyer, P. v. R.; Spitznagel, G. W. *J. Am. Chem. Soc.* **1983**, *105*, 5917.

(37) Gudat, D.; Haghverdi, A.; Nieger, M. *J. Organomet. Chem.* **2001**, *617*, 383.

(38) Schoeller, W. W.; Tubbesing, U. *J. Mol. Struct. (THEOCHEM)* **1995**, *343*, 49.

(39) Frisch, M. J.; et al. *Gaussian 03*, Revision B.04; Gaussian Inc.: Pittsburgh, PA, 2003.

ate α -aldimino-alimine **6** (25 mmol) and triethylamine (50 mmol) were dissolved in toluene (100 mL). The solution was cooled to $-78\text{ }^{\circ}\text{C}$ and PCl_3 (25 mmol) slowly added. The mixture was stirred for 36 h at room temperature. The precipitate was filtered off and washed twice with toluene (20 mL). Volatiles were evaporated in a vacuum, and the remaining residue was washed twice with *n*-hexane (30 mL). The products were obtained as pale yellow to brown solids.

(b) From Diazadienes. Lithium turnings (0.3 mol) were added to a solution of the appropriate diazadiene (0.15 mol) in THF (300 mL), and the mixture was stirred for 1 d under strict exclusion of oxygen. Excess lithium was then filtered off, the filtrate cooled to $-78\text{ }^{\circ}\text{C}$, and triethylamine hydrochloride (0.3 mol) added in several portions. When the addition was complete, the mixture was allowed to warm to room temperature and stirred for 1 h. After the mixture was cooled again to $-78\text{ }^{\circ}\text{C}$, PCl_3 (0.15 mol) was slowly added. The mixture was stirred for an additional 36 h at room temperature before all solvents were evaporated in a vacuum. The residue was transferred into a Soxhlet extraction apparatus and extracted with diethyl ether (350 mL) for 2 d. After completion of the extraction, volatiles were evaporated in a vacuum and the residue was washed twice with *n*-hexane (100 mL). The products were obtained as pale brown solids.

1,3-Bis(*tert*-butyl)-2-chloro-1,3,2-diazaphospholene¹³ (3c). Yield: 3.95 g (67%).

2-Chloro-1,3-bis(2,4,6-trimethylphenyl)-1,3,2-diazaphospholene²⁰ (3d). Yield: 5.70 g (70%). Elemental analysis: calcd C 66.94, H 6.74, N 7.81; found C 65.83, H 6.82, N 7.51.

2-Chloro-1,3-bis(2,6-diisopropylphenyl)-1,3,2-diazaphospholene (3e). Yield: 7.75 g (70%). Mp: $212\text{ }^{\circ}\text{C}$. $^1\text{H NMR}$ (C_6D_6): $\delta = 7.18$ (t, 2 H, $^3J_{\text{HH}} = 8.5$ Hz, p-CH), 7.12 (d, 4 H, $^3J_{\text{HH}} = 8.5$ Hz, m-CH), 6.21 (s, 2 H, N-CH), 3.74 (m, broad, 4 H, CH), 1.35 (d, 12 H, $^3J_{\text{HH}} = 6.8$ Hz, CH_3), 1.14 (d, 12 H, $^3J_{\text{HH}} = 6.8$ Hz, CH_3). $^{13}\text{C}\{^1\text{H}\}$ NMR (C_6D_6): $\delta = 146.6$ (i-C), 133.0 (o-C), 128.0 (p-CH), 123.4 (m-CH), 119.7 (d, $^2J_{\text{PC}} = 8.7$ Hz, N-CH), 27.7 (d, $^4J_{\text{PC}} = 2.3$ Hz, CH), 24.0 (CH_3), 23.2 (CH_3). $^{31}\text{P}\{^1\text{H}\}$ NMR (C_6D_6): $\delta = 141.0$. MS: *m/e* (relative intensity) = 442.2 ($[\text{M}]^+$, 6.4), 407.2 ($[\text{M} - \text{Cl}]^+$, 37.6), 162.1 ($[\text{M} - \text{C}_{14}\text{H}_{20}\text{N}_2\text{PCl}]^+$, 100.0). Elemental analysis for $\text{C}_{26}\text{H}_{36}\text{ClN}_2\text{P}$: calcd C 70.49, H 8.19, N 6.32; found C 67.44, H 8.74, N 5.88.

Preparation of 2-Hydrido-1,3,2-diazaphospholenes 1c–e. (a) By Using LiAlH_4 . A solution of **3e** (2.09 g, 5 mmol) in THF (50 mL) was cooled to $-78\text{ }^{\circ}\text{C}$, and a 1 M solution of LiAlH_4 in THF (1.25 mL, 1.25 mmol) was slowly added. The mixture was stirred for 30 min at $-78\text{ }^{\circ}\text{C}$ and then allowed to warm to room temperature. All solvents were evaporated in a vacuum, and then the residue was extracted with *n*-hexane (50 mL) and filtered. Concentration of the filtrate to a volume of 10 mL and storage at $-20\text{ }^{\circ}\text{C}$ produced yellow crystals which were collected by filtration and dried in a vacuum to yield 1.65 g (86%) of **1e**. Mp: $112\text{ }^{\circ}\text{C}$. $^1\text{H NMR}$ (C_6D_6): $\delta = 7.39$ (d, 1 H, $^1J_{\text{PH}} = 132.6$ Hz, PH), 7.16 (t, 2 H, $^3J_{\text{HH}} = 6.9$ Hz, p-CH), 7.14 (dd, 2 H, $^3J_{\text{HH}} = 6.9$ Hz, $^4J_{\text{HH}} = 3.2$ Hz, m-CH), 7.05 (dd, 2 H, $^3J_{\text{HH}} = 6.9$ Hz, $^4J_{\text{HH}} = 3.2$ Hz, m-CH), 5.91 (d, 2 H, $^3J_{\text{PH}} = 1.8$ Hz, N-CH), 3.69 (sept, 2 H, $^3J_{\text{HH}} = 6.9$ Hz, CH), 3.52 (sept, 2 H, $^3J_{\text{HH}} = 6.9$ Hz, CH), 1.35 (d, 6 H, $^3J_{\text{HH}} = 6.9$ Hz, CH_3), 1.26 (d, 6 H, $^3J_{\text{HH}} = 6.9$ Hz, CH_3), 1.19 (d, 6 H, $^3J_{\text{HH}} = 6.9$ Hz, CH_3), 1.13 (d, 6 H, $^3J_{\text{HH}} = 6.9$ Hz, CH_3). $^{13}\text{C}\{^1\text{H}\}$ NMR (C_6D_6): $\delta = 149.4$ (d, $^3J_{\text{PC}} = 2.4$ Hz, o-C), 148.3 (d, $^2J_{\text{PC}} = 2.9$ Hz, i-C), 137.6 (s, o-C), 137.4 (s, p-C), 124.0 (s, m-C), 123.7 (d, $^3J_{\text{PC}} = 1.6$ Hz, m-C), 122.5 (d, $^2J_{\text{PC}} = 6.3$ Hz, N-CH), 29.0 (s, CH), 28.3 (d, $^4J_{\text{PC}} = 1.3$ Hz, CH), 24.8 (s, CH_3), 24.5 (d, $^5J_{\text{PC}} = 1.6$ Hz, CH_3), 24.0 (d, $^5J_{\text{PC}} = 1.6$ Hz, CH_3), 23.4 (s, CH_3). ^{31}P NMR: $\delta = 71.6$ (d, $^1J_{\text{PH}} = 132.6$ Hz). MS: *m/e* (relative intensity) = 408.3 ($[\text{M}]^+$, 44.5), 407.3 ($[\text{M} - \text{H}]^+$, 100.0), 365.2 ($[\text{M} - \text{C}_3\text{H}_7]^+$, 4.8). Elemental analysis for $\text{C}_{26}\text{H}_{37}\text{N}_2\text{P}$: calcd C 76.43, H 9.13, N 6.86; found C 75.87, H 9.29, N 6.72.

(b) By Using “Red-Al”. A solution of the appropriate chloro-diazaphospholene **3c–e** (5 mmol) in THF (50 mL) was cooled to $-78\text{ }^{\circ}\text{C}$ and a 3.5 M solution of sodium dihydrido-bis(2-methoxyethoxy)-aluminate in toluene (0.7 mL, 2.5 mmol) slowly added. The mixture

was warmed to room temperature and stirred for 1 h. Solvents were evaporated in a vacuum, and then the residue was dissolved in hexane (50 mL) and filtered. The product was obtained after fractionated distillation of the filtrate in a vacuum (1c) or concentration of the filtrate in a vacuum and crystallization at $-20\text{ }^{\circ}\text{C}$. Following this procedure, **1c¹⁰** was obtained as a yellow oil with a yield of 0.77 g (77%).

Reaction of 1c with 2-Methoxybenzaldehyde. **1c** (200 mg, 1 mmol) was added to a solution of the aldehyde (136 mg, 1 mmol) in THF (10 mL) and the reaction stirred for 1 h at room temperature. The solvent was evaporated in a vacuum and the residue dissolved in acetonitrile (10 mL). Crystallization at $-28\text{ }^{\circ}\text{C}$ afforded **8** as a white powder that was collected by filtration and dried in a vacuum. Yield: 240 mg (65%). $^1\text{H NMR}$ (CD_3CN): $\delta = 6.90$ – 7.30 (m, 4 H, H_{phenyl}), 6.18 (d, 2 H, $^3J_{\text{PH}} = 1.9$ Hz, N-CH), 4.26 (d, 2 H, $^3J_{\text{PH}} = 4.3$ Hz, CH_2), 3.79 (s, 3 H, OCH_3), 1.42 (d, 2 H, $^4J_{\text{PH}} = 1.1$ Hz, CH_3). $^{13}\text{C}\{^1\text{H}\}$ NMR (CD_3CN): $\delta = 156.5$ (o-C), 135.7 (i-C), 128.1 (m-C), 127.8 (o-C), 127.4 (p-C), 119.8 (p-C), 112.0 (d, $^2J_{\text{PC}} = 9.7$ Hz, N-CH), 67.0 (OCH_3), 58.0 (d, $^2J_{\text{PC}} = 3.9$ Hz, C), 52.4 (d, $^2J_{\text{PC}} = 15.8$ Hz, CH_2), 30.0 (d, $^3J_{\text{PC}} = 10.3$ Hz, CH_3). $^{31}\text{P}\{^1\text{H}\}$ NMR (CD_3CN): $\delta = 92.7$. MS: *m/z* (relative intensity) = 336 ($[\text{M}]^+$, 78), 199 ($[\text{M} - \text{C}_8\text{H}_9\text{O}_2]^+$, 38), 159 ($[\text{M} - \text{C}_{11}\text{H}_{13}\text{O}_2]^+$, 85), 104 ($[\text{M} - \text{C}_{11}\text{H}_{13}\text{N}_2\text{OP}]^+$, 100). Elemental analysis for $\text{C}_{18}\text{H}_{29}\text{N}_2\text{O}_2\text{P}$ calcd: C 64.27, H 8.69, N 8.33; found: C 63.89, H 8.38, N 8.34.

Reaction of 1c with Benzophenone. **1c** (200 mg, 1 mmol) was added to a solution of benzophenone (182 mg, 1 mmol) in THF (10 mL) and the mixture stirred for 1 h at ambient temperature. The solvent was then evaporated in a vacuum and the residue dissolved in acetonitrile (5 mL). Diethyl ether (2 mL) was added and the solution stored at $-28\text{ }^{\circ}\text{C}$ until **10** precipitated as a white powder that was collected by filtration and dried in a vacuum. Yield: 280 mg (67%). $^1\text{H NMR}$ (C_6D_6): $\delta = 7.43$ (d, 4 H, $^3J_{\text{HH}} = 7.0$ Hz, o-CH), 6.90 – 7.20 (m, 12 H, p/m-CH), 5.97 (d, 2 H, $^3J_{\text{PH}} = 1.9$ Hz, CH), 5.54 (d, 1 H, $^3J_{\text{PH}} = 9.8$ Hz, O-CH), 1.13 (d, 2 H, $^4J_{\text{PH}} = 0.9$ Hz, CH_3). $^{13}\text{C}\{^1\text{H}\}$ NMR (C_6D_6): $\delta = 144.2$ (i-C), 128.8 (m-C), 128.2 (o-C), 125.5 (p-C), 111.8 (d, $^2J_{\text{PC}} = 9.8$ Hz, N-CH), 75.8 (d, $^2J_{\text{PC}} = 5.1$ Hz, O-CH), 51.8 (d, $^2J_{\text{PC}} = 3.9$ Hz, C), 29.2 (d, $^3J_{\text{PC}} = 9.7$ Hz, CH_3). $^{31}\text{P}\{^1\text{H}\}$ NMR (C_6D_6): $\delta = 96.4$.

Reactions of 1c with Acetophenone, Butyraldehyde, trans-Cinnamaldehyde, and Pentan-3-one. In an NMR tube equipped with a Teflon-sealed screw cap, the carbonyl compound (0.25 mmol) was dissolved in benzene-*d*₆ (0.6 mL), followed by addition of **1c** (50 mg, 0.25 mmol). The tube was closed and the reaction monitored by NMR spectroscopy. The products **9**, **11a,b** (relative ratio 3:1), **13**, and **14**, respectively, and the hydrolysis product **7¹⁶** were identified by 1D and 2D NMR studies.

Data for 9. $^1\text{H NMR}$: $\delta = 5.94$ (d, 2 H, $^3J_{\text{PH}} = 1.8$ Hz, N-CH), 3.26 (dt, 1 H, $^2J_{\text{PH}} = 4.8$ Hz, $^3J_{\text{PH}} = 6.3$ Hz, OCH), 1.46 (dt, 2 H, $^3J_{\text{PH}} = 6.3$ Hz, $^3J_{\text{PH}} = 7.2$ Hz, CH_2), 1.32 (tq, 2 H, $^3J_{\text{PH}} = 7.5$ Hz, $^3J_{\text{PH}} = 7.2$ Hz, CH_2), 1.31 (s, 18 H, CH_3), 0.83 (t, 3 H, $^3J_{\text{HH}} = 7.5$ Hz, CH_3). $^{13}\text{C}\{^1\text{H}\}$ NMR: $\delta = 112.6$ (d, $^2J_{\text{PC}} = 9.6$ Hz, N-CH), 61.5 (d, $^2J_{\text{PC}} = 5.4$ Hz, N-CH), 53.1 (d, $^2J_{\text{PC}} = 17.0$ Hz, o-CH), 34.2 (d, $^3J_{\text{PC}} = 1.7$ Hz, CH_3), 31.3 (d, $^3J_{\text{PC}} = 10.1$ Hz, CH_2), 30.1 (d, $^4J_{\text{PC}} = 4.0$ Hz, CH_2), 20.1 (s, CH_3). $^{31}\text{P}\{^1\text{H}\}$ NMR: $\delta = 93.1$.

Data for 11a. $^1\text{H NMR}$: $\delta = 7.24$ – 6.99 (m, 5 H, H_{phenyl}), 6.15 (ddt, 1 H, $^3J_{\text{PH}} = 10.1$ Hz, $^3J_{\text{HH}} = 6.1$ Hz, $^6J_{\text{HH}} = 1.5$ Hz, CH), 5.96 (d, 2 H, $^3J_{\text{PH}} = 1.9$ Hz, NCH), 4.69 (ddt, 1 H, $^3J_{\text{HH}} = 7.4$ Hz, $^3J_{\text{HH}} = 6.1$ Hz, $^4J_{\text{PH}} = 1.9$ Hz, CH), 3.54 (d, 2 H, $^3J_{\text{HH}} = 7.5$ Hz, CH_2), 1.31 (s, 18 H, CH_3). $^{31}\text{P}\{^1\text{H}\}$ NMR: $\delta = 95.0$.

Data for 11b. $^1\text{H NMR}$: $\delta = 7.24$ – 6.99 (m, 5 H, H_{phenyl}), 6.13 (d, 1 H, $^3J_{\text{HH}} = 12.1$ Hz, CH), 5.98 (d, 2 H, $^3J_{\text{PH}} = 1.8$ Hz, NCH), 5.27 (dt, 1 H, $^3J_{\text{HH}} = 12.1$ Hz, $^3J_{\text{HH}} = 7.4$ Hz, CH), 3.13 (d, 2 H, $^3J_{\text{HH}} = 7.4$ Hz, CH_2), 1.30 (s, 18 H, CH_3). $^{31}\text{P}\{^1\text{H}\}$ NMR: $\delta = 93.5$.

Data for 13. $^1\text{H NMR}$: $\delta = 7.74$ (dd, 2 H, $^3J_{\text{HH}} = 8.5$ Hz, $^4J_{\text{HH}} = 1.4$ Hz, o-CH), 7.12 (t, 1 H, $^3J_{\text{HH}} = 7.5$ Hz, p-CH), 7.05 (dd, 2 H, $^3J_{\text{HH}} = 8.5$ Hz, $^3J_{\text{HH}} = 7.5$ Hz, p-CH), 5.99 (dd, 1 H, $^3J_{\text{PH}} = 1.9$ Hz, $^3J_{\text{HH}} = 2.9$ Hz, N-CH), 5.84 (dd, 1 H, $^3J_{\text{PH}} = 1.7$ Hz, $^3J_{\text{HH}} = 2.9$ Hz,

N-CH), 4.61 (dq, 1 H, $^3J_{\text{PH}} = 9.7$ Hz, $^3J_{\text{HH}} = 6.5$ Hz, O-CH), 1.37 (d, 3 H, $^3J_{\text{HH}} = 6.5$ Hz, CH₃), 1.31 (d, 9H, $^4J_{\text{PH}} = 0.9$ Hz, CH₃), 1.13 (d, 9H, $^4J_{\text{PH}} = 0.8$ Hz, CH₃). $^{13}\text{C}\{^1\text{H}\}$ NMR: $\delta = 146.6$ (s, i-C), 127.8 (s, o-CH), 126.5 (s, p-CH), 125.7 (s, m-CH), 112.6 (d, $^2J_{\text{PC}} = 9.2$ Hz, N-CH), 112.5 (d, $^2J_{\text{PC}} = 9.2$ Hz, N-CH), 71.1 (d, $^2J_{\text{PC}} = 4.0$ Hz, OCH), 52.8 (d, $^2J_{\text{PC}} = 8.2$ Hz, N-C), 52.7 (d, $^2J_{\text{PC}} = 8.0$ Hz, N-C), 30.6 (d, $^3J_{\text{PC}} = 10.1$ Hz, CH₃), 30.1 (d, $^3J_{\text{PC}} = 10.1$ Hz, CH₃), 29.6 (d, $^3J_{\text{PC}} = 4.2$ Hz, CH₃). $^{31}\text{P}\{^1\text{H}\}$ NMR: $\delta = 97.0$.

Data for 14. ^1H NMR: $\delta = 5.88$ (d, 2 H, $^3J_{\text{PH}} = 1.9$ Hz, N-CH), 3.56 (dq, 1 H, $^3J_{\text{HH}} = 10.2$ Hz, $^3J_{\text{PH}} = 5.4$ Hz, O-CH), 1.49 (dq, 4 H, $^3J_{\text{HH}} = 10.2$ Hz, $^3J_{\text{HH}} = 7.5$ Hz, CH₂), 1.29 (s, 18 H, CH₃), 0.84 (t, 6 H, $^3J_{\text{HH}} = 7.5$ Hz, CH₃). $^{31}\text{P}\{^1\text{H}\}$ NMR: $\delta = 100.4$.

Reactions of 1c with ECl₄ (E = C, Si, Ge, Sn). In an NMR tube equipped with a Teflon-sealed screw cap, ECl₄ (0.5 mmol) was dissolved in acetonitrile-*d*₃ (0.6 mL). **1c** (100 mg, 0.5 mmol) was added, the tube closed, and the reaction monitored by NMR spectroscopy. The reaction products were identified in situ by 1D and 2D NMR studies.

Reaction with CCl₄. ^1H NMR: $\delta = 7.82$ (s, CHCl₃), 7.27 (s, 2 H, NCH, **3c**), 5.48 (s, CH₂Cl₂), 3.04 (CH₃Cl), 1.65 (d, 18 H, $^4J_{\text{PH}} = 1.8$ Hz, CH₃, **3c**). $^{13}\text{C}\{^1\text{H}\}$ NMR: $\delta = 122.3$ (s, **3c**), 78.2 (s, CHCl₃), 57.4 (s, **3c**), 54.0 (s, CH₂Cl₂), 29.1 (s, CH₃, **3c**), 26.8 (s, CH₃Cl). $^{31}\text{P}\{^1\text{H}\}$ NMR: $\delta = 173.0$ (**3c**).

Reaction with SiCl₄. ^1H NMR: $\delta = 7.33$ (s, 2H, CH, **3c**), 5.71 (s, SiHCl₃), 1.65 (s, 18 H, CH₃, **3c**). ^{29}Si NMR: $\delta = -10.6$ (d, $^1J_{\text{HSi}} = 379.6$ Hz, SiHCl₃). $^{31}\text{P}\{^1\text{H}\}$ NMR: $\delta = 176.3$ (**3c**).

Reaction with GeCl₄. **Data for 16c[GeCl₃].** ^1H NMR: $\delta = 8.24$ (s, 2 H, CH), 1.84 (d, 18 H, $^4J_{\text{HP}} = 1.8$ Hz, CH₃). $^{31}\text{P}\{^1\text{H}\}$ NMR: $\delta = 202.6$.

Reaction with SnCl₄. **Data for 16c[SnCl₃].** ^1H NMR: $\delta = 8.18$ (s, 2 H, CH), 1.71 (s, 18 H, CH₃). $^{31}\text{P}\{^1\text{H}\}$ NMR: $\delta = 205.0$. ^{119}Sn NMR (20 °C): $\delta = -42.0$.

Reaction of 3c with SnCl₂ and GeCl₂ x Dioxane. A solution of **3c** (1 mmol, 234 mg) and SnCl₂ (1 mmol, 190 mg) or GeCl₂ x dioxane (1 mmol, 232 mg), respectively, in CH₂Cl₂ (15 mL) was stirred for 1 h at room temperature. Addition of hexane (25 mL) produced a white precipitate which was collected by filtration and washed with hexane (10 mL).

Data for 16c[GeCl₃]. Yield: 348 mg (92%). ^1H NMR (CD₂Cl₂): $\delta = 8.24$ (s, 2 H, CH), 1.84 (s, 18 H, CH₃). $^{13}\text{C}\{^1\text{H}\}$ NMR (CD₂Cl₂): $\delta = 133.6$ (d, $^2J_{\text{PC}} = 3.6$ Hz, CH), 63.8 (d, $^2J_{\text{PC}} = 7.4$ Hz, NC), 32.1 (d, $^3J_{\text{PC}} = 9.4$ Hz, CH₃). $^{31}\text{P}\{^1\text{H}\}$ NMR (CD₂Cl₂): $\delta = 201.3$. Elemental analysis for C₁₀H₂₀Cl₃N₂PGe: calcd C 31.76, H 5.33, N 7.41; found C 30.56, H 5.11, N 6.96.

Data for 16c[SnCl₃]. Yield: 380 mg (90%). ^1H NMR (CD₂Cl₂): $\delta = 8.31$ (s, 2 H, CH), 1.85 (s, 18 H, CH₃). $^{13}\text{C}\{^1\text{H}\}$ NMR (CD₂Cl₂): $\delta = 132.4$ (d, $^2J_{\text{PC}} = 3.6$ Hz, CH), 62.2 (d, $^2J_{\text{PC}} = 7.8$ Hz, NC), 30.5 (d, $^3J_{\text{PC}} = 9.4$ Hz, CH₃). $^{31}\text{P}\{^1\text{H}\}$ NMR (CD₂Cl₂): $\delta = 199.4$. ^{119}Sn NMR (CD₂Cl₂, -20 °C): $\delta = -58.1$. Elemental analysis for C₁₀H₂₀Cl₃N₂-PSn: calcd C 28.31, H 4.75, N 6.60; found C 27.83, H 4.81, N 6.39.

Reaction of 1c with SnCl₂. Addition of **1c** (100 mg, 0.5 mmol) to a solution of SnCl₂ (95 mg, 0.5 mmol) in acetonitrile-*d*₃ (0.5 mL) led to immediate formation of a black precipitate which was filtered off and characterized as elemental tin by powder diffraction. The solution was transferred to a sure-sealed NMR tube and analyzed by ^1H and ^{31}P NMR spectroscopy. ^1H NMR: $\delta = 6.86$ (s, 2H, N-CH), 1.49 (s, 18 H, CH₃). $^{31}\text{P}\{^1\text{H}\}$ NMR: $\delta = 159.8$.

Reaction of 1c with Ph₂PCl. Chloro-diphenylphosphine (110 mg, 0.5 mmol) and **1c** (100 mg, 0.5 mmol) were dissolved in acetonitrile-*d*₃ (0.5 mL). The solution was analyzed by ^{31}P NMR spectroscopy. ^{31}P NMR: $\delta = 152.0$ (s, **3c**), -40.8 (d, $^1J_{\text{PH}} = 204.7$ Hz, Ph₂PH).

Reaction of 1c with 3c. **3c** (117 mg, 0.5 mmol) and **1c** (100 mg, 0.5 mmol) were dissolved in acetonitrile-*d*₃ (0.5 mL). The resulting solution was analyzed by ^1H and ^{31}P NMR spectroscopy and showed broadened signals attributable to **1c** and **3c**, respectively. Dynamic exchange between the two species was confirmed by a two-dimensional

^1H EXSY spectrum (see discussion in the text). ^1H NMR: $\delta = 6.69$ (broad s, 2 H, N-CH, **3c**), 6.03 (broad s, 2 H, N-CH, **1c**), 5.40 (broad s, 1 H, PH), 1.55 (broad s, 18 H, CH, **3c**), 1.22 (broad s, 18 H, CH₃, **1c**). $^{31}\text{P}\{^1\text{H}\}$ NMR: $\delta = 146.7$ (broad s, **3c**), 55.9 (broad s, **1c**).

Reaction of 1c with 16c[OTf]. **16c[OTf]** (174 mg, 0.5 mmol) and **1c** (100 mg, 0.5 mmol) were dissolved in acetonitrile-*d*₃ (1 mL), and the resulting mixture was analyzed by ^1H and ^{31}P NMR spectroscopy at temperatures between +50 and -40 °C. At the lowest temperature, a white solid precipitated which dissolved again upon warming. The variation of the spectral features and the conclusions drawn are discussed in the text. ^1H NMR (at 30 °C): $\delta = 5.55$ (s, N-CH), 4.87 (s, PH), 0.76 (s, CH₃). $^{31}\text{P}\{^1\text{H}\}$ NMR: $\delta = 99.4$ (broad).

Crystal Structure Determination of 1e, 16c[GeCl₃], and 16c[SnCl₃]. Data were collected on a Nonius Kappa CCD diffractometer at -150 °C using Mo K α radiation ($\lambda = 0.71073$ Å). The structures were solved by direct methods (SHELXS-97⁴⁰). Non-hydrogen atoms were refined anisotropically and H atoms with a riding model on F^2 (full-matrix least-squares, SHELXL-97⁴¹).

1e: yellow crystals, C₂₆H₃₇N₂P, $M = 408.6$, crystal size 0.40 × 0.30 × 0.20 mm³, monoclinic, space group $P2_1/n$ (No. 14), $a = 19.6744(3)$ Å, $b = 6.3916(1)$ Å, $c = 20.4343(4)$ Å, $\beta = 107.570(1)^\circ$, $V = 2449.75(7)$ Å³, $Z = 4$, $\rho(\text{calcd}) = 1.11$ Mg m⁻³, $F(000) = 888$, $\mu = 0.13$ mm⁻¹, 23 982 reflections measured, 4330 unique reflections ($R_{\text{int}} = 0.041$) used for structure solution and refinement with 265 parameters and 1 restraint, no absorption correction, $R1$ ($I > 2\sigma(I)$) = 0.038, $wR2 = 0.104$, largest differential peak and hole 0.399 and -0.288 e Å⁻³.

16c[GeCl₃]: orange crystals, C₁₀H₂₀Cl₃GeN₂P, $M = 378.2$, crystal size 0.55 × 0.50 × 0.40 mm³, orthorhombic, space group $Pnma$ (No. 62), $a = 12.9640(4)$ Å, $b = 17.3985(6)$ Å, $c = 7.3944(2)$ Å, $V = 1667.84(9)$ Å³, $Z = 4$, $\rho(\text{calcd}) = 1.51$ Mg m⁻³, $F(000) = 768$, $\mu = 2.40$ mm⁻¹, 7370 reflections measured, 1527 unique reflections ($R_{\text{int}} = 0.035$) used for structure solution and refinement with 82 parameters, empirical absorption correction with multiple reflections (maximum and minimum transmission 0.4125 and 0.3831), $R1$ ($I > 2\sigma(I)$) = 0.021, $wR2 = 0.051$, largest differential peak and hole 0.254 and -0.271 e Å⁻³.

16c[SnCl₃]: orange crystals, C₁₀H₂₀Cl₃N₂PSn, $M = 424.3$, crystal size 0.40 × 0.35 × 0.30 mm³, orthorhombic, space group $Pnma$ (No. 62), $a = 12.7132(3)$ Å, $b = 17.4583(5)$ Å, $c = 7.7723(2)$ Å, $V = 1725.07(8)$ Å³, $Z = 4$, $\rho(\text{calcd}) = 1.63$ Mg m⁻³, $F(000) = 840$, $\mu = 2.02$ mm⁻¹, 9453 reflections measured, 1574 unique reflections ($R_{\text{int}} = 0.036$) used for structure solution and refinement with 82 parameters, empirical absorption correction with multiple reflections (maximum and minimum transmission 0.5682 and 0.5375), $R1$ ($I > 2\sigma(I)$) = 0.020, $wR2 = 0.046$, largest differential peak and hole 0.441 and -0.490 e Å⁻³.

Acknowledgment. We thank Dr. U. Kessler, University of Bonn, for the powder diffraction measurements of tin samples.

Note Added after ASAP Publication. After this paper was published ASAP on March 3, 2006, Figure 1 was modified to properly display the thermal ellipsoids, as described in the caption. The corrected version was published ASAP on March 6, 2006.

Supporting Information Available: IR and Raman data for **16c[GeCl₃]** and **16c[SnCl₃]**; complete ref 40; computational details (extended geometric and energy data) (PDF); X-ray crystallographic data (CIF). This material is available free of charge via the Internet at <http://pubs.acs.org>.

JA057827J

(40) Sheldrick, G. M. *Acta Crystallogr.* **1990**, *A46*, 467.

(41) Sheldrick, G. M., University of Göttingen, 1997.